FEBS Letters 587 (2013) 3261–3266

FEBS Letters

journal homepage: www.FEBSLetters.org

Endoplasmic Reticulum stress reduces COPII vesicle formation and modifies Sec23a cycling at ERESs

Giuseppina Amodio [b], Rossella Venditti [c], Maria Antonietta De Matteis [c], Ornella Moltedo [b], Piero Pignataro [b], Paolo Remondelli [a,*]

[a] Dipartimento di Medicina e Chirurgia, Università degli Studi di Salerno, 84081 Baronissi, Salerno, Italy
[b] Dipartimento di Farmacia, Università degli Studi di Salerno, 84084 Fisciano, Salerno, Italy
[c] Telethon Institute for Genetics and Medicine, 80131 Naples, Italy

ARTICLE INFO

Article history:
Received 10 July 2013
Accepted 8 August 2013
Available online 27 August 2013

Edited by Felix Wieland

Keywords:
COPII
Sec23
ERES
ER stress

ABSTRACT

Exit from the Endoplasmic Reticulum (ER) of newly synthesized proteins is mediated by COPII vesicles that bud from the ER at the ER Exit Sites (ERESs). Disruption of ER homeostasis causes accumulation of unfolded and misfolded proteins in the ER. This condition is referred to as ER stress. Previously, we demonstrated that ER stress rapidly impairs the formation of COPII vesicles. Here, we show that membrane association of COPII components, and in particular of Sec23a, is impaired by ER stress-inducing agents suggesting the existence of a dynamic interplay between protein folding and COPII assembly at the ER.

1. Introduction

Protein and lipids exit the Endoplasmic Reticulum (ER) [1] in COPII coated vesicles budding from ER membrane domains called exit sites (ERES) or transitional ER (tER) [2–5]. COPII formation begins when the GTP exchange factor Sec12 converts the Sar1 GTPase into its GTP bound form. Sar1-GTP inserts its amphiphilic α-elix into the ER membrane [6,7], starts membrane bending and recruits the Sec23/Sec24 dimers forming the pre budding complex that engages cargo proteins interacting with Sec24 [8–11]. Finally, Sec13/Sec31 heterotetramers complete membrane curvature and COPII vesicle formation [12,13].

COPII function is regulated by distinct factors. During the initial steps, COPII assembly is organized by the ERES resident protein Sec16 that nucleates COPII formation by interacting with Sec23 [14] and Sar1 [15]. In addition, Sec16 stabilizes prebudding complexes by preventing Sec31 stimulation of Sec23 GAP activity [16,17].

Disassembly of COPII depends on Sec23 GAP activity on Sar1 GTPase [18,19], which is fully activated in the presence of Sec31.

COPII assembly is regulated by cargo proteins [20–23], and by other factors, such the ERES protein p125 [24], the Ca^{2+}-binding protein ALG2 [25], the TFG1 oncoprotein [26] and by post-translational modifications of its components [27].

ER stress is a perturbing condition that activates the Unfolded Protein Response (UPR) [28] pathway required to stimulate survival response to protein unfolding [29] or the cell death program [30]. Previously, we showed that thapsigargin, a powerful inducer of the ER stress, decreases transport of cargo proteins from the ER to the Golgi complex [31–34].

Here, we report that ER stress modifies COPII assembly by altering Sec23a cycling indicating the existence of feedback circuits between protein folding and COPII coat assembly at the ER.

2. Materials and methods

2.1. Cell cultures

Huh7 cells were grown in DMEM, 4.5 g/l D-glucose, 1 mM Na-pyruvate, 2 mM L-glutamine, 10% FCS. To induce ER stress, Huh7 cells were incubated with 300 nM thapsigargin (Sigma–Aldrich), 2 μM dithiothreitol, 10 μg/ml MG132 (Sigma–Aldrich).

2.2. Antibodies

Antibodies used were: anti-GM130 (BD Transduction Laboratories), anti-Sec31a [35], anti-KIAA0310 (Bethyl Laboratories), anti-Sar1 (Millipore); anti-Sec23a (ABR), anti-GAPDH and anti-calreti-

* Corresponding author. Address: Dipartimento di Medicina e Chirurgia, Università degli Studi di Salerno, Via S. Allende, I-84081 Baronissi, Salerno, Italy. Fax: +39 089 969602.
E-mail address: premondelli@unisa.it (P. Remondelli).

0014-5793/$36.00
http://dx.doi.org/10.1016/j.febslet.2013.08.021

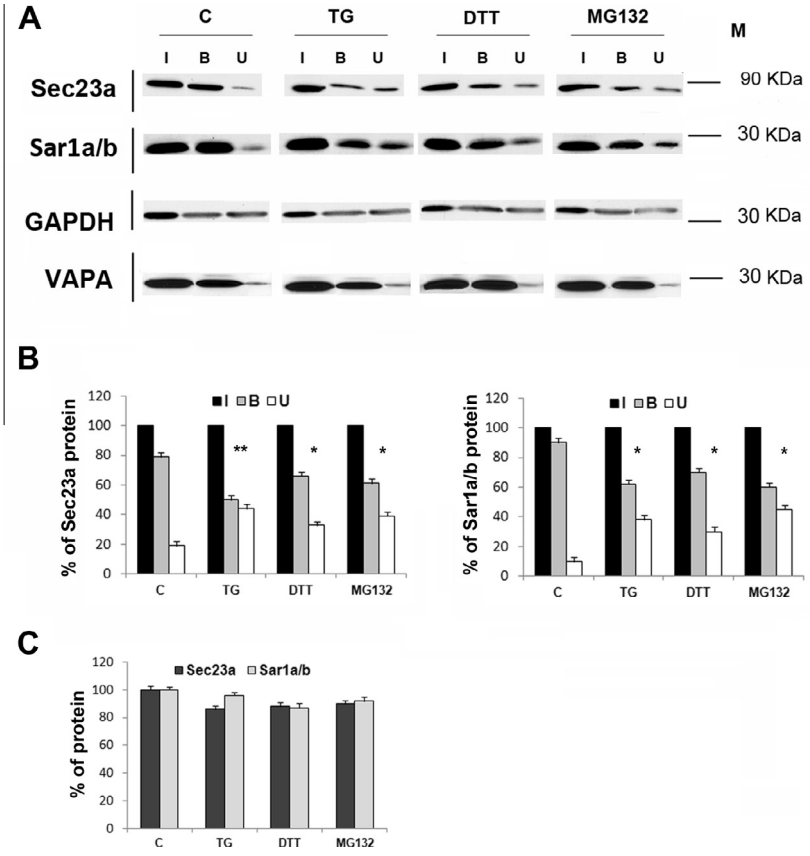

Fig. 1. Effect of the ER stress on the amount of membrane bound Sec23a and Sar1a/b proteins. (A) Control Huh7 cells (C) were treated with 300 nM TG, 2 mM DTT or 10 μg/ml MG132. Total cell lysates obtained from cells treated with inactive SLO (*input*: I), membrane fraction (*bound*: B) and cytosolic fraction (*unbound*: U) obtained by SLO-p cells were analysed by western blot with specific antibodies. GAPDH and VAPA were used as reference for cytosolic and vesicular proteins, respectively. One out of three separate experiments is shown. (B) Histograms show the percent of *input* (I) membrane *bound* (B) and *unbound* (U) Sec23a and Sar1a/b. Values obtained by densitometry of autoradiographs performed by the Image J program are the mean ± S.D. of three independent experiments. (C) Histograms show the relative abundance of Sec23a and Sar1a/b in the input samples calculated from densitometry of immunoblots represented in (A) using GAPDH as internal standard. Statistical analysis was performed using the Student *t*-test ($n = 6–9$). $^{*}P$-value $\leqslant 0.5$; $^{**}P$-value $\leqslant 0.1$.

culin (Sigma–Aldrich). FITC-, Texas Red- (Jackson Immuno Research Laboratories), TRITC- and CY5- (GE Healthcare) conjugated antibodies were used for immunofluorescence analyses; HRP-conjugated anti-IgG (Sigma–Aldrich) were used for immunoblotting analysis.

2.3. Streptolysin-O permeabilization assay

Streptolysin-O permeabilization (SLO-p) was performed as described [36] with some modifications. Streptolysin-O (SLO) toxin (0.8 U/ml) was preactivated (5 min at 37 °C) in SLO buffer (20 mM Hepes-KOH pH 7.2, 110 mM KOAc, 2 mM Mg(OAc)2, 1 mM DTT). Huh7 cells were washed with SB containing SLO and incubated 10 min 4 °C. Cells were washed at 4 °C with Transport Buffer (TB: 25 mM HEPES KOH, 2.5 mM Mg(OAc)2, 110 mM KOAc, 5 mM EGTA, 1.8 mM CaCl2, 100 mM ATP, 500 mM phosphocreatine, 1000 U/ml Creatine phosphokinase) and incubated 15 min at 37 °C to allow permeabilization (SLO-p cells) or at 4 °C to keep SLO inactivated (*input*) .

Total lysates (Tris–HCl 10 mM, NaCl 150 mM, EDTA pH 8.00 1 mM, 1% Triton X-100) of unpermeabilised cells (*input*), cytosolic proteins recovered from the incubation buffer (TB) (*unbound*) and membrane bound proteins recovered from cell lysates of adherent cells (*bound*) of SLO-p cells were subjected to SDS–PAGE and analyzed by Western Blot [37]. Cytosolic glyceraldehyde 3-phosphate dehydrogenase (GAPDH) and the 33 kDa membrane protein VAMP (vesicle-associated membrane protein)-associated protein (VAPA) were used to monitor SLO-p efficiency. The amount of *bound* and *unbound* proteins was measured by densitometry of auto-radiographs and referred as the percent of the *input* proteins. Values were the mean ± S.D. of three independent experiments. Statistical analysis was performed using the Student *t*-test ($n = 6–9$).

2.4. Immunofluorescence

SLO-p cells were fixed in PBS-4% paraformaldehyde and treated for 30 min with PBS containing 0.5% BSA and 50 mM NH_4Cl. Cells were incubated with anti-GM130 antibody that accessed exclusively SLO-p cells, successively treated with PBS-Saponin 1% and stained with the indicated primary antibodies. *Intact cells* incubated with inactivated (4 °C) SLO-p, fixed, treated with PBS-Saponin 1% and visualized with the indicated antibodies. Images were collected by LSM 510 Zeiss confocal microscopy. Fluorescence intensity in the region of interest was normalized for the fluorescence intensity obtained in an equal area of the Golgi complex labelled by the anti-GM130 antibody. In the Fig. 5, immunofluoresence was carried out as previously reported [34]. Co-localization of fluorescence signals was quantified by using the LSM 510 wizard. The number of co-localized pixels was normalized for the total fluorescent pixels in the image.

2.5. Transfection, Fluorescence Recovery after Photobleaching (FRAP) and Fluorescence Loss in Photobleaching (FLIP)

Huh7 cells grown on live cell dishes (Mattek) were transfected with 2 μg of GFP-Sec23a or GFP-Sec16a (kindly provided by Dr. D.J.

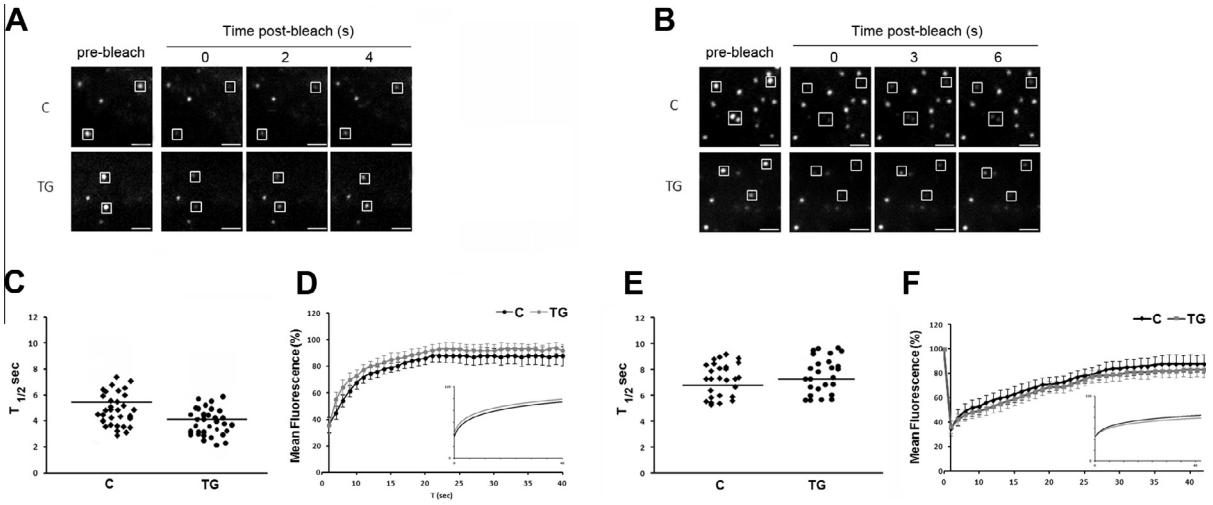

G

GFP-Sec23 a	Number	$T_{1/2}$	Immobile Fraction (%)	P-value
C	35	5.52 ± 1.5	12.75 ± 2.1	0.042
TG	35	4.45 ± 1.1	7.37 ± 2.3	

H

GFP-Sec16 a	Number	$T_{1/2}$	Immobile Fraction (%)	P-value
C	27	7.011 ± 1.5	11.11 ± 2.2	0.032
TG	27	7.629 ± 1.3	16.18 ± 2.5	

Fig. 2. Quantitative analysis of GFP-Sec23a and GFP-Sec16a Fluorescence Recovery After Photobleaching (FRAP). Huh7 cells were transfected with 2 μg of either GFP-Sec23a or GFP-Sec16a expressing vector. 24 h after transfection cells were analysed by FRAP while treated (TG) or not (C) with 300 nM TG for 2 h. Fluorescence of GFP-Sec23a (A) or GFP-Sec16a (B) from individual ERES is shown. Plots of individual *T½* values in seconds are reported for GFP-Sec23a (C) or GFP-Sec16a (E). Bars indicate the mean of *T½* values of individual ERES from 15 different cells. (D, F) Average recovery curve for GFP-Sec23a (D) and GFP-Sec16a (F). Insets show these data fitted to a single exponential. (G, H) Tables report the number of individual ERES analysed (*N*), the rate of fluorescence recovery in seconds (*T½*); the percent of GFP-Sec23a or GFP-Sec16a proteins bound to the membrane during post-bleach cycles (Immobile Fraction).

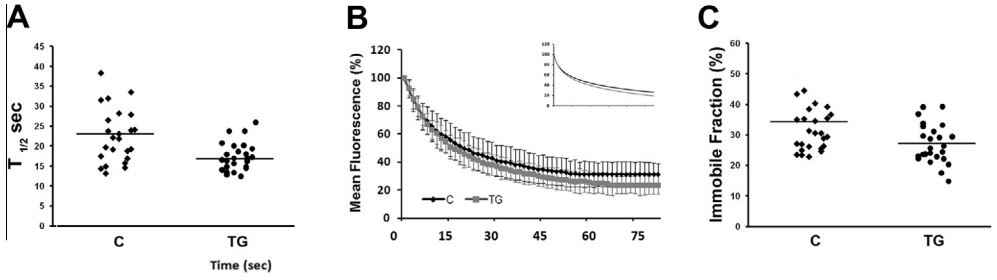

D

GFP-Sec23 a	Number	$T_{1/2}$	Immobile Fraction (%)	P-value
C	25	23.01 ± 4.3	32.7 ± 6.2	0.0017
TG	25	17.52 ± 1.78	27.3 ± 5.6	

Fig. 3. Quantitative analysis of GFP-Sec23a Fluorescence Loss In Photobleaching (FLIP). Huh7 cells were transfected with 2 μg of GFP-Sec23a expressing vector. 24 h after transfection cells were analysed by FLIP while treated (TG) or not (C) with 300 nM TG for 2 h. Plots of individual *T½* values (A) and immobile fraction (C) of individual 25 ERES from 15 different cells. Bars indicate the mean of *T½* values or immobile fraction. (B) Averaged FLIP curve for the 25 ERES analyzed. The inset shows this curve fitted to a single exponential. (D) Table shows the number of individual ERES analysed (*N*), the rate of fluorescence loss in seconds (T ½); the percent of GFP-Sec23a protein remaining bound to the membrane during post-bleach cycles (Immobile Fraction).

Stephens; Department of Biochemistry, University of Bristol) plasmid using Fugene 6 (Roche). 24 h after transfection, cells were imaged [38] with Zeiss LSM 510 META scanning confocal microscope enclosed in a heated box in DMEM, supplemented with 30 mM HEPES, pH 7.4 and 10% FCS. For FRAP measurements a 63× 1.4 NA Plan-Apochromat objective was used. Photobleaching was performed on individual Sec16a or Sec23a spots with five iterations of the 488 laser at 100% AOTF power. Post bleaching images were collected for 40 s, 1 frame every 1 s and twofold line averaging. Fluorescence recovery was quantified using Zeiss LSM 510 FRAP Wizard and exported for analysis to Microsoft excel. Recycling kinetics were obtained by curve fitting to a one phase exponential $f(t) = A \times (1 - e^{-kt}) + B$, where, A is the mobile fraction, B is the fluorescence directly after photo bleaching (%), and k is the rate of fluorescence recovery from which $t½$ is determined [$t½ = \ln(2)/k$].

For FLIP analysis, a region of 8 × 8 μm encompassing about 40% of the cytoplasm was intermittently photo bleached with 488 laser at 100% AOTF power. Fluorescence loss was measured from individual Sec16a or Sec23a spots for 80 s outside of the bleached area.

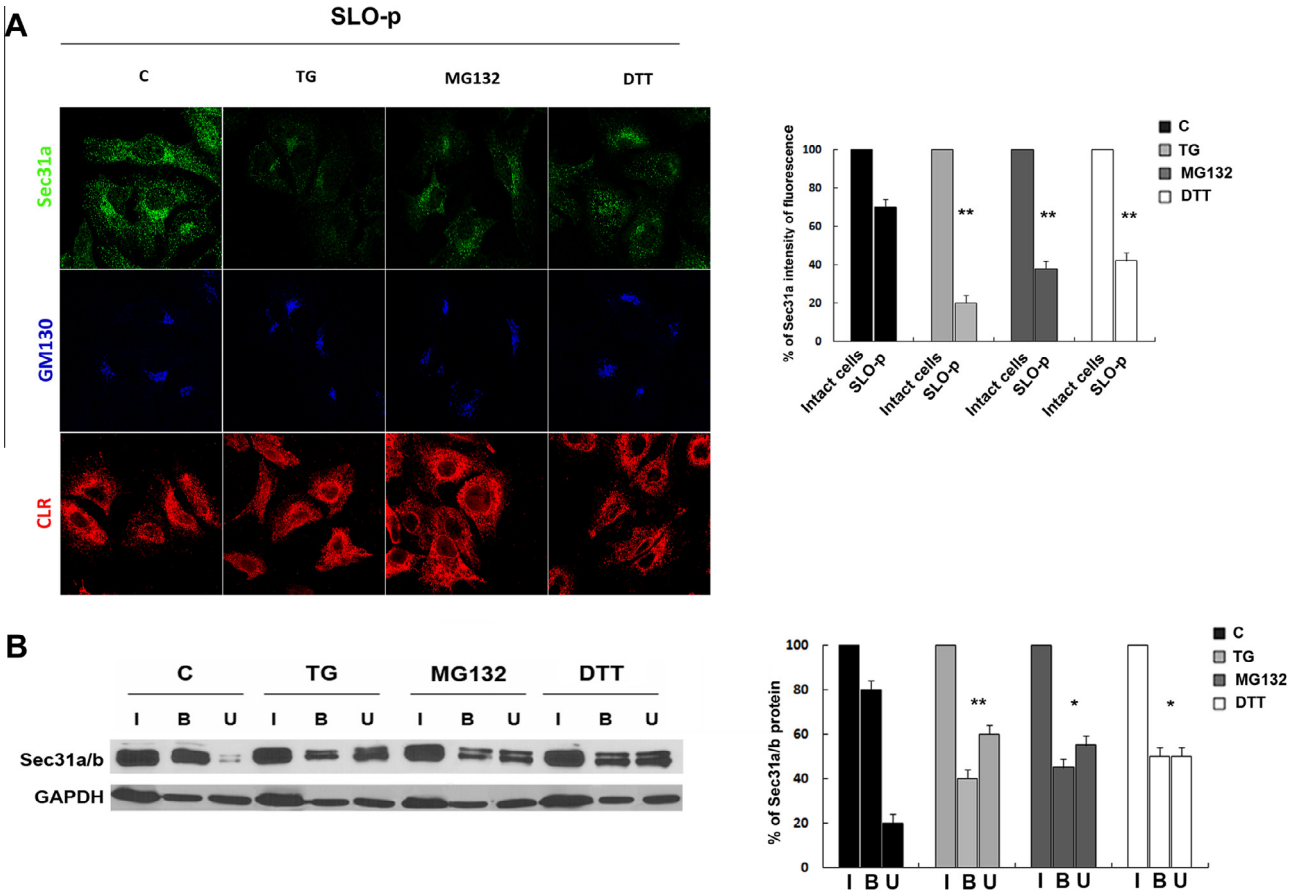

Fig. 4. Analysis of membrane bound Sec31a in SLO permeabilized Huh7 cells. (A) SLO-p Huh7 control cells (C) or cells treated for 1 h with 300 nM TG, 2 mM DTT or 10 μg/ml MG132 were fixed and co-labelled by immunofluorescence with anti-Sec31a and anti-GM130 antibodies as indicated. In the same experimental conditions, SLO-p cells were stained with the ER marker calreticulin (CLR). Histograms show the percent of Sec31a held on membranes normalized for GM130 mean intensity of fluorescence in SLO-p cells. Intact cells were fixed, permeabilized with PBS-1% saponin and stained for GM130 and Sec31a proteins. For each condition, a minimum of 100 different cells were analysed in three independent experiments. (B) Western blot analysis of Sec31a/b in SLO-p Huh7 cells. Total cell extracts (*input*: I), membrane fraction (*bound*: B) and cytosolic fraction (*unbound*: U) were analysed by western blot with anti Sec31a/b antibody. Histogram shows the percent membrane bound (B) and unbound (U) Sec31a/b. The mean ± S.D. of three independent experiments is reported. Statistical analysis was performed using the Student *t*-test ($n = 6–9$) described in the methods section $^{*}P$-value $\leqslant 0.5$; $^{**}P$-value $\leqslant 0.1$.

Five different cells and for each cell five sec23a spots were analysed and quantified as for FRAP experiments. Statistical significance was determined using standard deviation and the Student's unpaired *t*-test.

3. Results

3.1. ER stress reduces membrane bound Sec23a

To investigate the effect of ER stress on COPII assembly Huh7 cells were treated with 300 nM thapsigargin (TG) or 2 μM DTT or 10 μg/ml MG132, three different ER-stress inducers that act via distinct mechanisms (Fig. 1). The amount of membrane bound Sec23a or both Sar1a and Sar1b was measured in SLO-p cells as described in the Methods section. Our experiments showed that, compared to control cells, membrane retained Sec23a in SLO-p cells was reduced by 50 ± 3% in TG-treated cells, 66 ± 2.9 in DTT- or 61 ± 2.1% in MG132-treated cells (Fig. 1B). Albeit at lesser extent, we observed reduced membrane association of Sar1a/b proteins (TG = 62 ± 3.1; DTT = 70 ± 2.9 and MG132 = 60 ± 3.0) (Fig. 1B). Instead, the intracellular level of either Sec23a and Sar1a/b was not modified (Fig. 1C) suggesting that ER stress could affect membrane stability of COPII components.

3.2. ER stress accelerates Sec23a cycling

Next, we performed FRAP measurements [21] for GFP-Sec23a from individual ERES by using TG, as representative inducer of ER stress (Fig. 2A). In agreement with previous results [21,38], FRAP assays revealed that GFP-Sec23a cycles at ERES of control cells with a $T_{1/2}$ of 5.52 ± 1.5 s (Fig. 2C and G). Instead, GFP-Sec23a cycled more rapidly in TG treated cells ($T_{1/2} = 4.45 \pm 1.1$ s). This result was statistically significant ($P = 0.042$) and indicated a faster turnover of GFP-Sec23a at ERESs of ER stressed cells. Additionally, FRAP results confirmed that TG reduced membrane bound GFP-Sec23a (see Fig. 2G: GFP-Sec23a, immobile fraction).

In contrast, GFP-Sec-16a cycling exhibited similar rate in control and in TG-treated cells ($T_{1/2} = 7.011 \pm 1.5$ s and $T_{1/2} = 7.6 \pm 1.3$ s, respectively), indicating that membrane association of Sec16a is not affected by ER stress (Fig. 2B, E and H). Moreover, Sec16a was stably bound to membranes as shown by the higher percentage of immobile GFP-Sec16a compared to GFP-Sec23a (see Fig. 2H: GFP-Sec16a, immobile fraction).

Finally, to further define the effect of ER stress on Sec23a cycling, we performed FLIP measurements of GFP-Sec23a fluorescence at individual ERES (Fig. 3). Fluorescence loss measured outside of bleached regions showed that GFP-Sec23a fluorescence

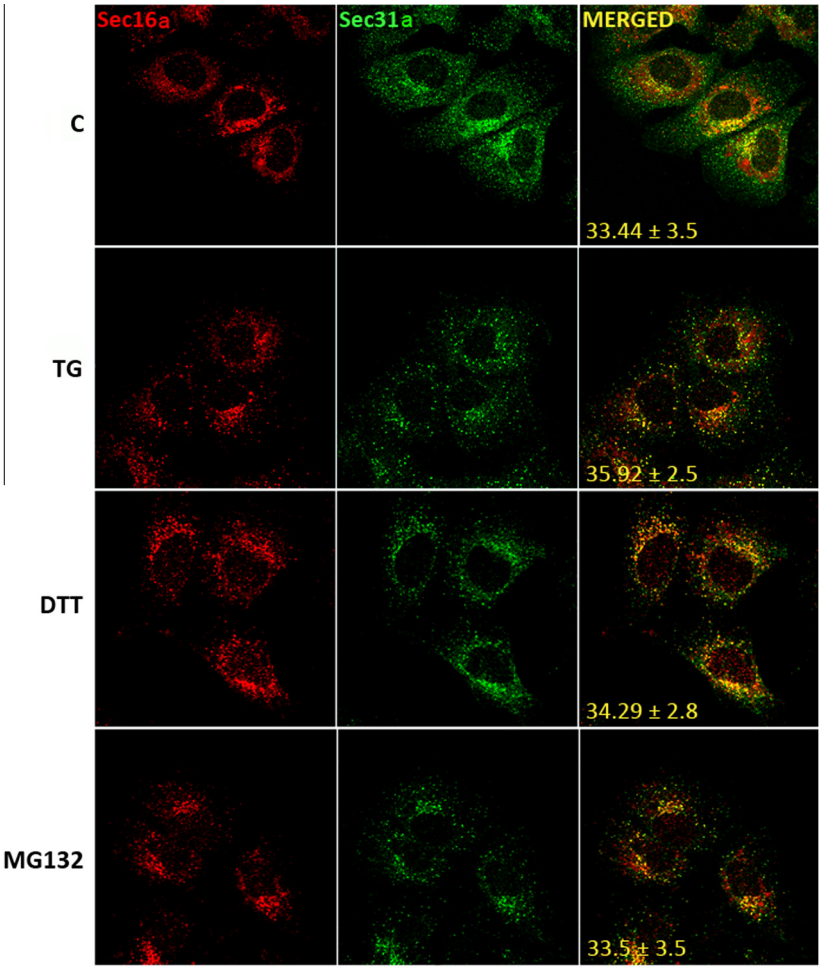

Fig. 5. Immunofluorescence analysis of Sec31a and Sec16a distribution in unstressed or ER stressed cells. Huh7 cells seeded on glass cover slips were either untreated (C) or treated with 300 nM TG for 2 h, 2 mM DTT or 10 μg/ml MG132, fixed and analyzed by immunofluorescence with the anti-Sec16a (Sec16a) and anti-Sec31a (Sec31a) antibodies. Percent of Sec31a pixels colabeling with Sec16a pixels is shown on the right.

declined faster in the TG-treated cells starting with a $T_{1/2}$ = 23.01 ± 4.3 in the control cells to $T_{1/2}$ = 17.52 ± 1.78 in TG-treated cells (Fig. 3A and D) suggesting that ER stress could induce Sec23a release.

3.3. ER stress alters the association of Sec31a to intracellular membrane

Next, to further evaluate the effect of ER stress on COPII assembly, we analysed the association of Sec31a with intracellular membranes. Sec31a retained at Huh7 endomembranes was measured by immunofluorescence in SLO-p cells, either in presence or in absence of TG or DTT or MG132 (Fig. 4A).

Semiquantitative results revealed that, with respect to control cells, TG (20 ± 3.8%) and, at lower extent, MG132 (38 ± 3.9%) and DTT (42 ± 4.0%), reduced membrane bound Sec31a confirming that ER stress restrains COPII assembly (Fig. 4A). Notably, neither SLO-p nor exposure to stress induced ER morphology changes as revealed by the ER marker calreticulin (Fig. 4A). Moreover, semi-quantitative immunofluorescence analysis was confirmed by WB analysis of SLO-p cells (Fig. 4B), which revealed, in line with immunufluoresence results, that the amount of bound Sec31a/b in the ER stressed cells declined to 40 ± 3.9%, 45 ± 4.0% and 50 ± 4.1% in the TG, MG132 and DTT treated cells, respectively (Fig. 4B).

Finally, we compared the intracellular distribution of Sec31a to that of the endogenous Sec16a protein before and following exposure of Huh7 cells to TG or DTT or MG132 (Fig. 5). As we expected from our previous results [34], fluorescence intensity of Sec31a spots declined in the stress induced cells compared to control cells, being 44.3 ± 3.3% in the TG-, 73.6 ± 12.3% DTT- and 53.1 ± 5.9% in the MG132-induced cells (Fig. 5). Instead, ER stress did not induce changes on the intracellular pattern of Sec16a, which instead co-localized with Sec31a in the ER stressed cells at the same extent as in control cells, suggesting that Sec16a normally nucleates COPII assembly at ERESs (Fig. 5).

4. Discussion

In this work, we tried to gain insight on the molecular events underlying the control of COPII assembly during ER stress. To this aim, we examined the effect of ER stress by the parallel use of distinct ER-stress inducers on the intracellular distribution and membrane association of proteins having different roles in COPII assembly.

Our data show that ER stress induces reduced stability of COPII components. Such an effect is particularly evident on Sec23, which plays a crucial role in the formation of prebudding complexes, in the coat assembly and in the COPII disassembly throughout its GAP activity on Sar1 [19]. Therefore, reduced COPII vesicle formation during ER stress could be simply explained by reduced Sec23 stability and/or by delayed COPII turnover due to insufficient Sec23 GAP activity on Sar1.

On the other hand, vesicle bound Sec23 interacts with the tethering factor TRAPPI to ensure directionality of ER to Golgi transport [39,40]. Sec23a, as suggested by FLIP assay, is rapidly released from intracellular membranes of ER stressed cells leading to reduced Sec23/TRAPP interactions. Subsequently, reduced Sec23/TRAPP complexes would certainly reduce tethering and fusion events required for efficient cargo transport thus reducing transport of cargo proteins as we observe in ER stressed cells [34].

In yeast cells, a Golgi-associated kinase, (CK1δ orthologue) phosphorylates Sec23p within the Sec23p/Sec24p complex [40] indicating that phosphorylation is needed for vesicle budding. Furthermore yeast Sec23p undergoes to ubiquitination/de-ubiquitination cycles and this balance is essential for a proper secretory function [41]. Hence, the question arises as to whether ER stress, presumably throughout the UPR, would induce similar Sec23 modifications to regulate COPII assembly in mammalian cells.

In conclusion, our results enforce the hypothesis that COPII assembly plays central role throughout the ER stress response by preventing post-ER compartments from the accumulation of misfolded proteins that could more efficiently either refold in the ER or be destined to degradation through the ERAD.

Acknowledgments

This work was supported by the University of Salerno (FARB 2009 and FARB 2010) to PR. MADM acknowledges the support of Telethon Grant number GSP08002 and GGP06166, AIRC, Grant IG 8623, and of Programma Operativo Nazionale (PON) 01_00862.

References

[1] Watson, P., Townley, A.K., Koka, P., Palmer, K.J. and Stephens, D.J. (2006) Sec16 defines endoplasmic reticulum exit sites and is required for secretory cargo export in mammalian cells. Traffic 7, 1678–1687.
[2] Palade, G. (1975) Intracellular aspects of the process of protein synthesis. Science 189, 347–358.
[3] Orci, L., Ravazzola, M., Meda, P., Holcomb, C., Moore, H.P., Hicke, L. and Schekman, R. (1991) Mammalian Sec23p homologue is restricted to the endoplasmic reticulum transitional cytoplasm. Proc. Natl. Acad. Sci. USA 88, 8611–8615.
[4] Bannykh, S.I., Rowe, T. and Balch, W.E. (1996) The organization of endoplasmic reticulum export complexes. J. Cell Biol. 135, 19–35.
[5] Aridor, M. and Balch, W.E. (1996) Principles of selective transport: coat complexes hold the key. Trends Cell Biol. 6, 315–320.
[6] Barlowe, C. and Schekman, R. (1993) SEC12 encodes a guanine-nucleotide-exchange factor essential for transport vesicle budding from the ER. Nature 365, 347–349.
[7] Weissman, J.T., Aridor, M. and Balch, W.E. (2001) Purification and properties of rat liver Sec23–Sec24 complex. Methods Enzymol. 329, 431–438.
[8] Miller, E., Antonny, B., Hamamoto, S. and Schekman, R. (2002) Cargo selection into COPII vesicles is driven by the Sec24p subunit. EMBO J. 21, 6105–6113.
[9] Lee, M.C., Orci, L., Hamamoto, S., Futai, E., Ravazzola, M. and Schekman, R. (2005) Sar1p N-terminal helix initiates membrane curvature and completes the fission of a COPII vesicle. Cell 122, 605–617.
[10] Hicke, L., Yoshihisa, T. and Schekman, R. (1992) Sec23p and a novel 105-kDa protein function as a multimeric complex to promote vesicle budding and protein transport from the endoplasmic reticulum. Mol. Biol. Cell 3, 667–676.
[11] Barlowe, C. et al. (1994) COPII: a membrane coat formed by Sec proteins that drive vesicle budding from the endoplasmic reticulum. Cell 77, 895–907.
[12] Fath, S., Mancias, J.D., Bi, X. and Goldberg, J. (2007) Structure and organization of coat proteins in the COPII cage. Cell 129, 1325–1336.
[13] Stagg, S.M., LaPointe, P., Razvi, A., Gurkan, C., Potter, C.S., Carragher, B. and Balch, W.E. (2008) Structural basis for cargo regulation of COPII coat assembly. Cell 134, 474–484.
[14] Espenshade, P., Gimeno, R.E., Holzmacher, E., Teung, P. and Kaiser, C.A. (1995) Yeast SEC16 gene encodes a multidomain vesicle coat protein that interacts with Sec23p. J. Cell Biol. 131, 311–324.
[15] Supek, F., Madden, D.T., Hamamoto, S., Orci, L. and Schekman, R. (2002) Sec16p potentiates the action of COPII proteins to bud transport vesicles. J. Cell Biol. 158, 1029–1038.
[16] Kung, L.F. et al. (2012) Sec24p and Sec16p cooperate to regulate the GTP cycle of the COPII coat. EMBO J. 31, 1014–1027.
[17] Yorimitsu, T. and Sato, K. (2012) Insights into structural and regulatory roles of Sec16 in COPII vesicle formation at ER exit sites. Mol. Biol. Cell 23, 2930–2942.
[18] Bielli, A., Haney, C.J., Gabreski, G., Watkins, S.C., Bannykh, S.I. and Aridor, M. (2005) Regulation of Sar1 NH2 terminus by GTP binding and hydrolysis promotes membrane deformation to control COPII vesicle fission. J. Cell Biol. 171, 919–924.
[19] Yoshihisa, T., Barlowe, C. and Schekman, R. (1993) Requirement for a GTPase-activating protein in vesicle budding from the endoplasmic reticulum. Science 259, 1466–1468.
[20] Matsuoka, K., Orci, L., Amherdt, M., Bednarek, S.Y., Hamamoto, S., Schekman, R. and Yeung, T. (1998) COPII-coated vesicle formation reconstituted with purified coat proteins and chemically defined liposomes. Cell 93, 263–275.
[21] Forster, R., Weiss, M., Zimmermann, T., Reynaud, E.G., Verissimo, F., Stephens, D.J. and Pepperkok, R. (2006) Secretory cargo regulates the turnover of COPII subunits at single ER exit sites. Curr. Biol. 16, 173–179.
[22] Farhan, H., Weiss, M., Tani, K., Kaufman, R.J. and Hauri, H.P. (2008) Adaptation of endoplasmic reticulum exit sites to acute and chronic increases in cargo load. EMBO J. 27, 2043–2054.
[23] Tabata, K.V., Sato, K., Ide, T., Nishizaka, T., Nakano, A. and Noji, H. (2009) Visualization of cargo concentration by COPII minimal machinery in a planar lipid membrane. EMBO J. 28, 3279–3289.
[24] Shimoi, W. et al. (2005) P125 is localized in endoplasmic reticulum exit sites and involved in their organization. J. Biol. Chem. 280, 10141–10148.
[25] Shibata, H., Suzuki, H., Yoshida, H. and Maki, M. (2007) ALG-2 directly binds Sec31A and localizes at endoplasmic reticulum exit sites in a Ca2+-dependent manner. Biochem. Biophys. Res. Commun. 353, 756–763.
[26] Witte, K. et al. (2011) TFG-1 function in protein secretion and oncogenesis. Nat. Cell Biol. 13, 550–558.
[27] Barlowe, C.K. and Miller, E.A. (2013) Secretory protein biogenesis and traffic in the early secretory pathway. Genetics 193, 383–410.
[28] Ron, D. and Walter, P. (2007) Signal integration in the endoplasmic reticulum unfolded protein response. Nat. Rev. Mol. Cell Biol. 8, 519–529.
[29] Schroder, M. and Kaufman, R.J. (2005) ER stress and the unfolded protein response. Mutat. Res. 569, 29–63.
[30] Tabas, I. and Ron, D. (2011) Integrating the mechanisms of apoptosis induced by endoplasmic reticulum stress. Nat. Cell Biol. 13, 184–190.
[31] Spatuzza, C., Renna, M., Faraonio, R., Cardinali, G., Martire, G., Bonatti, S. and Remondelli, P. (2004) Heat shock induces preferential translation of ERGIC-53 and affects its recycling pathway. J. Biol. Chem. 279, 42535–42544.
[32] Renna, M., Faraonio, R., Bonatti, S., De Stefano, D., Carnuccio, R., Tajana, G. and Remondelli, P. (2006) Nitric oxide-induced endoplasmic reticulum stress activates the expression of cargo receptor proteins and alters the glycoprotein transport to the Golgi complex. Int. J. Biochem. Cell Biol. 38, 2040–2048.
[33] Renna, M., Caporaso, M.G., Bonatti, S., Kaufman, R.J. and Remondelli, P. (2007) Regulation of ERGIC-53 gene transcription in response to endoplasmic reticulum stress. J. Biol. Chem. 282, 22499–22512.
[34] Amodio, G. et al. (2009) Endoplasmic reticulum stress reduces the export from the ER and alters the architecture of post-ER compartments. Int. J. Biochem. Cell Biol. 41, 2511–2521.
[35] Marra, P. et al. (2001) The GM130 and GRASP65 Golgi proteins cycle through and define a subdomain of the intermediate compartment. Nat. Cell Biol. 3, 1101–1113.
[36] De Matteis, M.A., Santini, G., Kahn, R.A., Di Tullio, G. and Luini, A. (1993) Receptor and protein kinase C-mediated regulation of ARF binding to the Golgi complex. Nature 364, 818–821.
[37] Amodio, G., Moltedo, O., Monteleone, F., D'Ambrosio, C., Scaloni, A., Remondelli, P. and Zambrano, N. (2011) Proteomic signatures in thapsigargin-treated hepatoma cells. Chem. Res. Toxicol. 24, 1215–1222.
[38] Hughes, H. et al. (2009) Organisation of human ER-exit sites: requirements for the localisation of Sec16 to transitional ER. J. Cell Sci. 122, 2924–2934.
[39] Cai, H. et al. (2007) TRAPPI tethers COPII vesicles by binding the coat subunit Sec23. Nature 445, 941–944.
[40] Lord, C., Bhandari, D., Menon, S., Ghassemian, M., Nycz, D., Hay, J., Ghosh, P. and Ferro-Novick, S. (2011) Sequential interactions with Sec23 control the direction of vesicle traffic. Nature 473, 181–186.
[41] Cohen, M., Stutz, F., Belgareh, N., Haguenauer-Tsapis, R. and Dargemont, C. (2003) Ubp3 requires a cofactor, Bre5, to specifically de-ubiquitinate the COPII protein, Sec23. Nat. Cell Biol. 5, 661–667.